ELSEVIER

Journal of Hazardous Materials 46 (1996) 197–213

JOURNAL OF HAZARDOUS MATERIALS

The boiling liquid collapsed bubble explosion (BLCBE): A preliminary model

C.M. Yu[1], J.E.S. Venart*

Fire Science Centre, University of New Brunswick, Fredericton, NB, Canada E3B 5A3

Received 5 May 1995; accepted 27 January 1995

Abstract

A preliminary physical and mathematical model (along with its associated computer code) has been developed to describe the behaviour of the BLCBE. The transient thermo-hydraulic behaviour of a vertical cylindrical vessel containing a pressure liquefied gas (propane) at 1 MPa initial pressure and 90% initial fill has been simulated with a crack suddenly opening up in the vapour space. Eulerian and Lagrangian coordinate systems have been used to numerically model the time-dependent behaviour of the vapour and liquid regions, respectively. Analyses of the propagation of the depressurization wave (caused by the mass discharge through the crack) and the recompressive wave (caused by the rise in the liquid–vapour interface (due to void generation)), permit the pressure, density and velocity fields in the vapour region and the void fraction and pressure distributions in the liquid region to be predicted.

Keywords: PLG vessel failures; BLCBE; BLEVE

1. Introduction

The loss of containment (LOC) of pressure liquefied gas (PLG) vessels under accidental fire engulfment or with mechanical failure (gland/seal loss, sample line breakage, fatigue or corrosion) is extremely complex [1–4]. The LOC depends upon: (i) the extent and intensity of external heating, (ii) the type and size of initial thermal or mechanical failure, (iii) the pressure relief device (PRD) operation and flare (if contents flammable), (iv) The fluid and fill level, (v) the thermohydraulic history of the commodity prior to its initial failure, and (vi) the construction of the pressure vessel.

* Corresponding author. Tel.: 506-453-4509. Fax: 506-453-5025.

[1] Permanent address: Department of Thermal Engineering, University of Science and Technology Beijing, Beijing 10083, China.

SSDI 0304-3894(95)00071-2

Previously the most severe failure event for these vessels has been termed the boiling liquid expanding vapour explosion (BLEVE) [4, 5]. This type of incident is purported to be caused by a total LOC and the release of the PLG contents in an adiabatic flash. For propane, under normal storage conditions, this results in a 40% to 50% flash vapour fraction with the auto-refrigerated evaporating residue distributed as large droplets or left in the form of a pool. The reason for the total LOC is, however, not explained by this process.

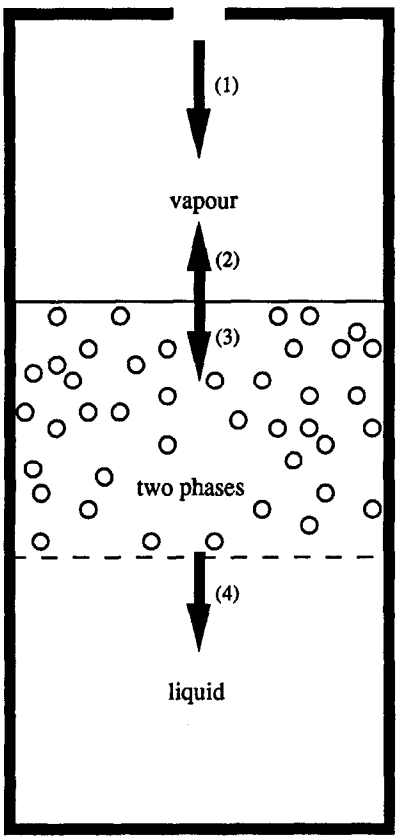

Fig. 1. Schematic diagram of BLEVE/BLCBE process as in a vessel: (1) propagation of the vapour depressurization wave caused by mass discharge through a crack; (2) propagation of the compressive wave caused by the rise in the interface (in the vapour region); (3) propagation of vapour depressurization wave caused by mass discharge through the crack and the compressive wave caused by rise of the two-phase interface; (4) propagation of interface between the two-phase and the liquid space.

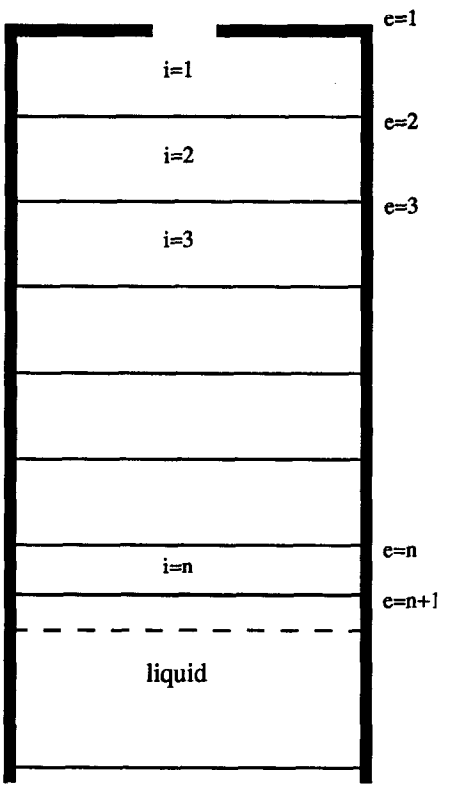

Fig. 2. Discretization of the vapour space.

Another type of incident has recently [6] been proposed to explain some of the more severe BLEVE type industrial incidents reported. The cause for this LOC has been termed a boiling liquid compressed bubble explosion (BLCBE) and results from a complex multi-step adaptive and coherent bubble formation-growth-collapse process in a pressure liquefied gas *and* its interaction with the containment vessel. The main features of the event are (i) a partial vessel failure (i.e., a 'sub-critical' sized crack or opening), (ii) the rapid depressurization of an already nucleated and now superheated liquid, (iii) rapid bubble growth and then the constraint of the expanding two-phase system (by either physical, acoustic, or inertial means), (iv) the repressurization, back to nearly the original containment pressure (or values in excess) followed by, (v) adaptive and coherent bubble collapse resulting in the formation of a power amplified liquid shock wave. This results in (vi) wall–pressure wave interactions causing the total and rapid vessel destruction, with (vii) an explosive mechanical distribution of the liquid contents as a finely divided aerosol, and (viii) heat transfer and total evaporation (and if flammable, auto-ignition) of the aerosol. The bubble growth and collapse phenomena results in a power amplification of the bubble energy and hence dynamic pressures which may greatly exceed the original thermodynamic containment pressure dictated by its original temperature. The local bubble collapse process can be likened to a process of coherent cavitation.

In this paper a partial and preliminary mathematical-physical model of the BLCBE process described above will be detailed along with its associated computer code.

2. Mathematical-physical model

2.1. Preliminaries

An amount of liquid at temperature T_0 is contained in a closed cylindrical vessel at its associated saturated vapour pressure p_0. A crack of area, A_C, suddenly opens up in the vapour region. A depressurization wave then commences propagation from the crack towards the vapour–liquid interface at the speed of sound in the vapour phase (Fig. 1(1)). After this depressurization wave crosses the liquid interface, it propagates into the liquid at the speed of sound in the liquid towards the bottom of the vessel (Fig. 1(3)). During this period, the depressurization wavefront divides the liquid into two parts (Fig. 1(4)); a portion that has not been disturbed and is still at its saturated pressure and temperature, and that portion which is depressurized (and now superheated) with some fraction of it transformed into vapour by bubble formation. As a consequence of this latter process the liquid–vapour interface rapidly swells and thus compresses the vapour region above to a higher pressure; this compressive wave is propagated into both the vapour (Fig. 1(2)) and the two-phase regions (Fig. 1(3)).

This rapid rise in vapour pressure, due to recompression, may be one reason for vessel failure since the crack size may now become 'critical'. Another possible reason is that the swelled liquid, which has large momentum and thus dynamic energy, can impact at the top of the vessel and therefore also cause unstable crack extension. The interface fluid is, however, two-phase and its constraint, by either the repressurization

or by its physical containment could result in coherent bubble collapse and thus provide a further opportunity for energy release with its conversion into a local dynamic pressure (i.e. coherent cavitation).

For convenience and discussion this analysis is restricted to the vertical one-dimensional cylindrical system shown in Fig. 1. Propane, is contained in a vessel taken to be 4.5 cm diameter and 20 cm height. Its initial temperature is 27 °C (1 MPa). The initial fill was taken as 90%. A crack of 1 cm^2 suddenly ($t \geqslant 0$) appears at the centre of the top of the vessel. The crack size remains constant in time.

2.2. *Pressure propagation in the vapour region*

The mass flow rate discharged from the crack can be taken to be

$$\frac{dm}{dt} = C_d A_C C. \tag{1}$$

Here, ρ and C are the density and velocity of fluid through the opening of area A_C. Obviously, C's extreme value is the velocity of sound at local conditions.

The discharge of vapour through the hole results in a change in its density and so a density field, with its associated velocity field, will be created in the vapour region. These should obey the conservation equations of mass and momentum;

$$\frac{\partial \rho}{\partial t} + \frac{\partial \rho u}{\partial x} = 0, \tag{2}$$

$$\frac{\partial u}{\partial t} + u\frac{\partial u}{\partial x} = -\frac{1}{\rho}\frac{\partial p}{\partial x} + \mu\frac{\partial^2 u}{\partial x^2}. \tag{3}$$

The vapour pressure field can reasonably be considered to be proportional to the vapour density field under an isothermal expansion or compression condition, i.e.

$$p \sim \rho. \tag{4}$$

Eqs. (2)–(4) can be discreted in an Eulerian coordinate system as shown with Fig. 2.

$$\rho_1^{n+1} = \rho_i^n - \frac{\Delta t}{\Delta x}[(\rho u)_{e+1}^{n+1} - (\rho u)_e^{n+1}], \tag{5}$$

$$\frac{u_e^{n+1} - u_e^n}{\Delta t} + u_e^{n+1}\frac{u_{e+1}^{n+1} - u_e^{n+1}}{\Delta x} = -\frac{1}{\rho_i^{n+1}}\frac{p_i^{n+1} - p_{i-1}^{n+1}}{\Delta x}, \tag{6}$$

$$p_i^{n+1} = p_i^n \frac{\rho_i^{n+1}}{\rho_i^n}. \tag{7}$$

The choice of time step length, Δt, and space length step, Δx, should satisfy the requirements for local sound velocity propagation, i.e.

$$C = \Delta x/\Delta t. \tag{8}$$

An iterative method is used to solve the resulting set of non-linear algebraic equations, Eqs. (5)–(7), for p_i^{n+1}, ρ_i^{n+1} and u_e^{n+1}.

2.3. Pressure and void fraction distribution in the liquid phase

It is known that free gas is always present in a real liquid as small bubbles or nuclei. There are usually 10^4–10^8 bubbles contained in a cubic centimetre for most liquids [7, 8]. For propane, those bubbles with a critical radius of say less than 1 μm give a volume concentration of bubbles ranging between 10^{-11} and 10^{-7}. When pressure is locally suddenly reduced these bubbles rapidly grow. In addition some new bubbles will also be initiated as a result of the local liquid superheat.

Bubble growth is mainly governed by two mechanisms: (1) dynamics and (2) heat transfer. Inertial bubble growth, obtained by solving the momentum equation for the bubble, yields a time-dependent bubble radius of [6, 7]:

$$R_{\text{in}} = 1.0929 \sqrt{\Delta p/\rho_l}\, t, \tag{9}$$

where Δp represents the pressure drop causing the liquid superheat and ρ_l is the density of the liquid.

Heat and mass transfer from the superheated liquid to the bubble also drives its thermal growth and this may be obtained from [6, 7]:

$$R_{\text{t}} = \frac{2\Delta T\sqrt{3\rho_l C_{\text{p}} k/\pi}}{\rho_{\text{v}} h_{\text{fg}}} \sqrt{t}, \tag{10}$$

where h_{fg} is the latent heat, C_{p} is the specific heat, k the liquid thermal conductivity, and ρ_{v} the vapour density.

The relationships between R_{in} and R_{t} are shown in Fig. 3 for various degrees of superheat. Obviously the crossover between inertial and thermal growth occurs at very small superheat and bubble size.

It is extremely difficult to exactly determine the number of bubbles generated due to a depressurization event in a real liquid since this is dependent upon bubble nuclei and impurities present. In order to analyse and estimate the generation rate of bubbles, J, in the depressurized superheated liquid the following expression may be utilized [8]:

$$J = 3.37 \times 10^{35} \left(\frac{\rho_l^2 \sigma}{M^3 B}\right)^{0.5} \exp\left(\frac{-1.182 \times 10^5 \sigma^3}{T \Delta p^2}\right), \tag{11}$$

where B is a constant and M the molecular weight.

It is obvious from Eq. (11) that the surface tension, σ, and pressure drop, Δp, associated with the liquid superheat as well as the temperature of the liquid are very important factors influencing the rate of bubble generation. Fig. 4 shows the dependence of bubble generation rate on superheat temperature associated with a pressure drop.

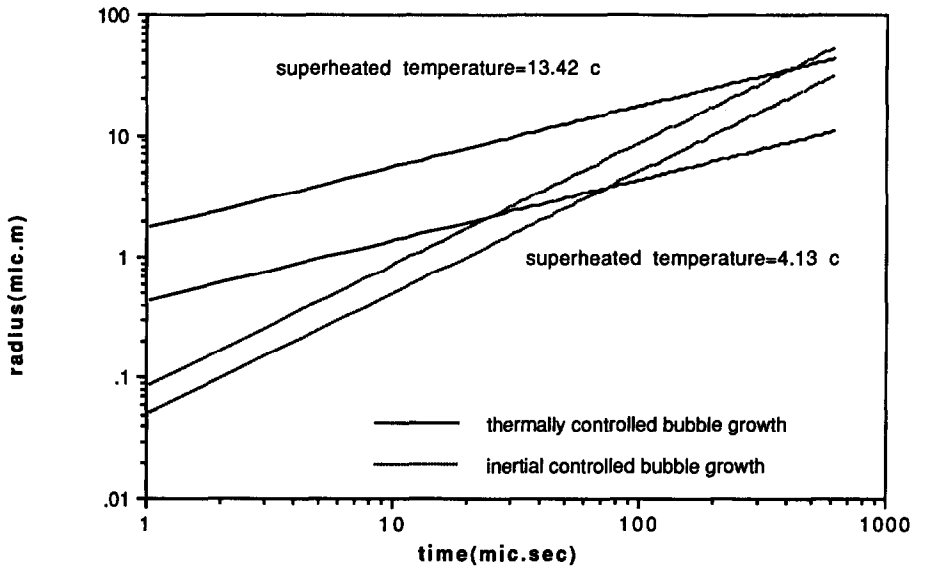

Fig. 3. Bubble growth in superheated liquid propane.

In order to model the swelled two-phase region, a Lagrangian coordinate system has been adopted as shown in Fig. 5. The size of each discrete control volume is variable with time but its mass is always constant. Pressure signals can thus propagate across the liquid–vapour interface as well as between neighbouring control volumes. The propation velocity for these pressures is therefore directly determined by the speed of sound, $C_{2\phi}$, for each control volume of void fraction, α. The two-phase speed of sound is [7]:

$$C_{2\phi} = \sqrt{\frac{\rho_l}{\alpha(1-\alpha)}}. \tag{12}$$

The calculation of the void fraction in each control volume is based on its known pressure and the associated size and number of the bubbles present at any instant in time.

In order to calculate the maximum possible dynamic pressure caused by bubble collapse the following expression has been adopted [6]:

$$P_{\mathrm{dyn}} = E_{\mathrm{b}} V_{\mathrm{s}} / C_{2\phi} t_{\mathrm{in}} A_{\mathrm{s}},$$

where E_{b} represents the internal energy content of the bubbles per unit volume, A_{s} and V_{s} are the interior surface area and system volume, respectively, t_{in} represents the time during which the bubble collapse occurs as determined from the appropriate inertial growth curve for a particular bubble size.

3. Results and discussion

A numerical analysis based upon the processes above will now be discussed for the described case. Figs. 6(a)–(d) shows the calculated local vapour velocities and pressure distributions as a function of depth in the vessel at selected times.

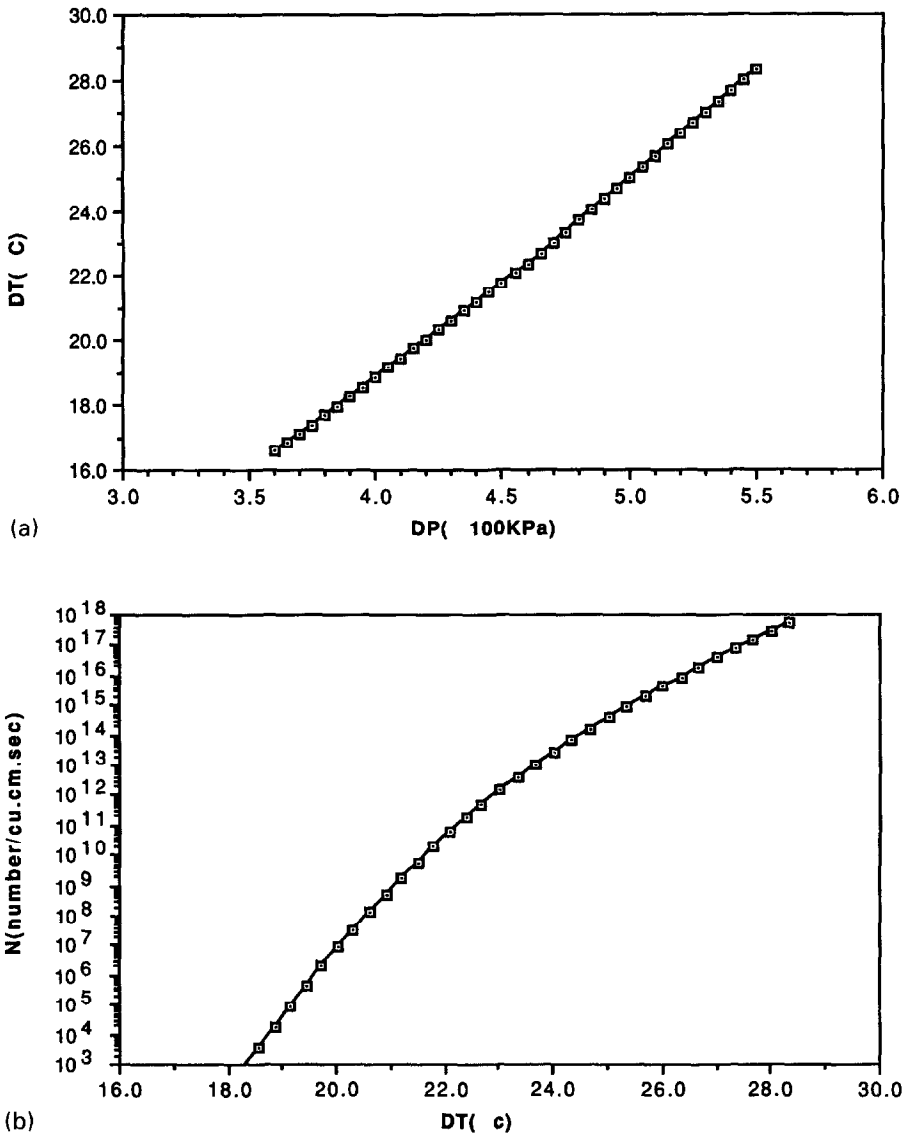

Fig. 4. Relationship between (a) pressure drop and superheat temperature, (b) generation rate of bubble and superheat temperature.

Fig. 6(a) is at a time (~ 64 μs) when the vapour depressurization wave has just reached the vapour–liquid interface. The local vapour pressure drop resulting from the crack opening at $t = 0$ causes the vapour to accelerate towards the opening with increasing velocity.

In Fig. 6(b) (~ 380 μs) the depressurization wave has now proceeded into the liquid resulting in local liquid superheats which, for the number of initial bubble nuclei present ($N_b = 0.1 \times 10^7$ bubbles/cm^3), are insufficient to result in the generation of new bubbles or the growth of existing nuclei. The interface level, as a result, does not move and the vapour continues to be accelerated towards the opening.

Fig. 6(c) at ~ 745 μs, in addition to illustrating the continuing depressurization of the liquid, now shows the commencing influence of the bubble generation and growth. The two-phase interface rapidly swells and accelerates towards the opening commencing a recompression of the vapour space.

In Fig. 6(d), the last time step prior to interface impact on the upper vessel wall (780 μs), the vapour pressure is already greater than twice the original containment pressure. The vapour velocity is in excess of 250 m/s.

Figs. 7 and 8 illustrate the void fraction developing in the vessel as a result of bubble growth from the original nuclei determined in the calculations for Fig. 6.

In Fig. 7 the void fraction history at three depths is shown over the time span 600–800 μs. Due to local superheat the generation of new bubbles and growth of existing bubbles (curve (a)) is very rapid and much more pronounced at the interface than in the middle of the vessel (curve (b)). There has obviously been no void generated at the bottom of the vessel (curve (c)).

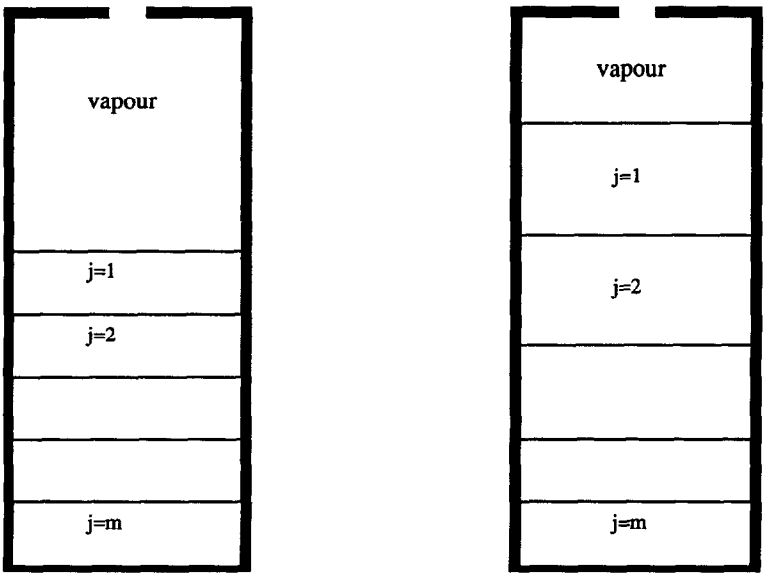

Fig. 5. Discretization of the liquid region.

In curve (a), the vapour compressive wave, caused by the interacting dynamics of the two-phase swell and vapour recompression, results in some reduction of bubble size with time.

Fig. 8 shows the void fraction distribution as a function of position at several different times. The times represented by curves (1) and (2) are the same as for Fig. 6(c) and (d). The significant difference between these is that the void fraction at the top

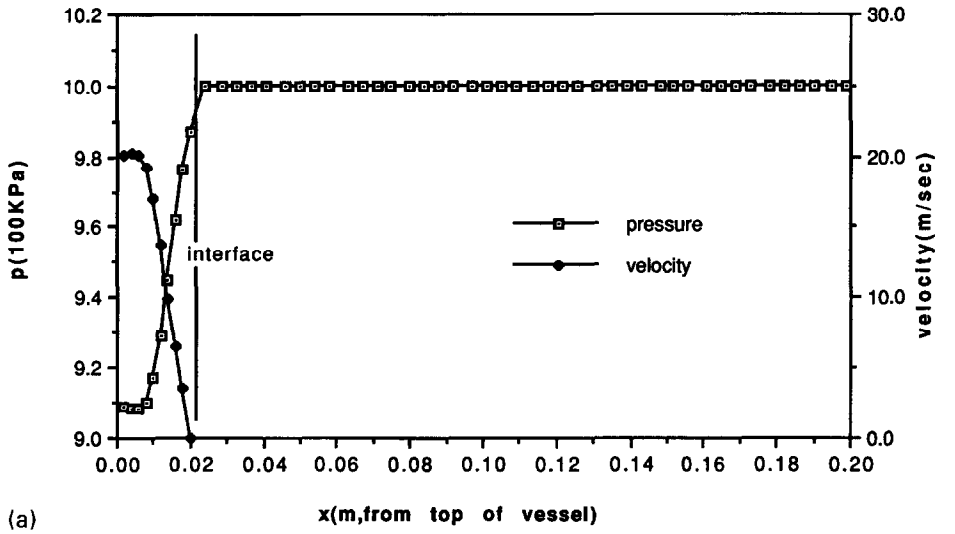

(a)

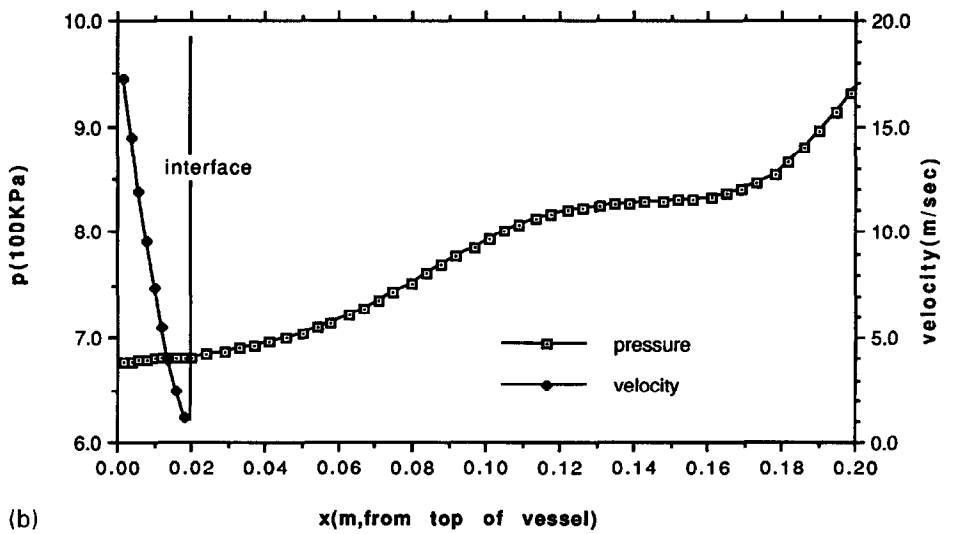

(b)

Fig. 6. (a) Distribution of vapour velocity and pressure in the vessel: (a) 63.8 μs, (b) 383 μs, (c) 745 μs, (d) 780 μs.

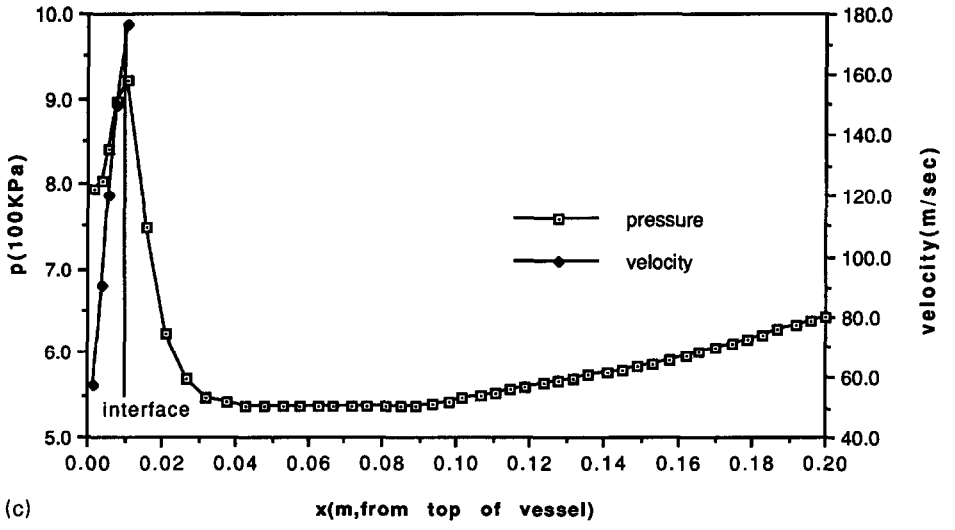

(c)

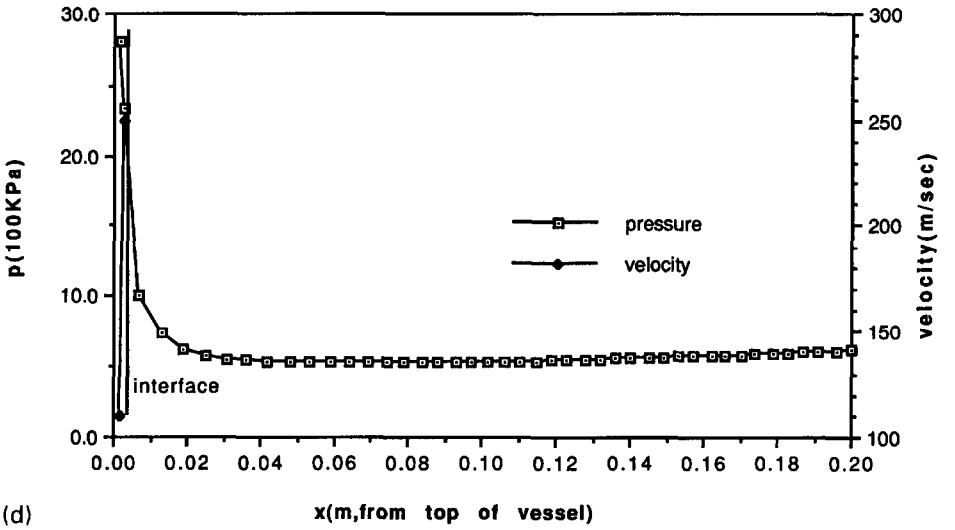

(d)

Fig. 6. Continued.

location is smaller than at earlier times due to the vapour recompression at the interface. The maximum value of the curve appears at an intermediate location in the swelled fluid.

Fig. 9 shows the variation with time of interface height and velocity (Fig. 9(a)) and top most vapour pressure, Fig. 9(b). It should be noted that the dynamic pressure generated by the impact of the liquid interface can be interpreted as a water hammer

effect and, in itself, may be sufficient to damage the vessel. The vapour pressure at the top of the vessel is shown in Fig. 9(b) and this also, or in conjunction with the interface impact, may damage the already weakened vessel.

A subsequent calculation with a greater number of original bubbles than before ($N_b = 0.43 \times 10^7 > 0.1 \times 10^7$ bubbles/cm^3), but with a volume concentration still less than 10^6, provides the results shown in Figs. 10 and 11.

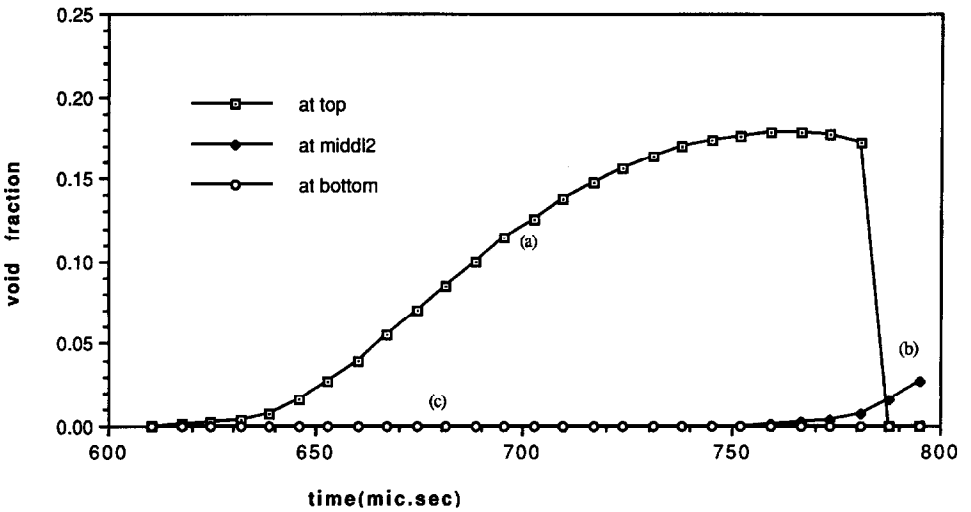

Fig. 7. Void fraction development at top, middle and bottom locations of the liquid region.

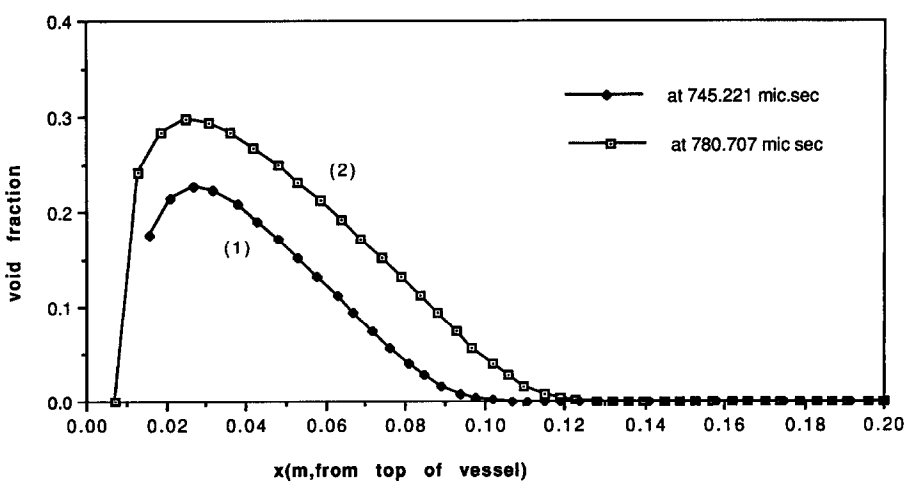

Fig. 8. Distribution of void fraction in the liquid region at two times.

The time variation of interface height and velocity for this new condition is shown in Fig. 10(a) along with the pressure experienced at the top of the vessel (Fig. 10(b)). Due to the greater number of original bubbles interface levels rise earlier and much more gently than for Fig. 9(a). The interface velocity is greatly reduced and its response rate is significantly lower than the previous case. As a consequence the events are much slower and cause a much lower and more gentle vapour recompression

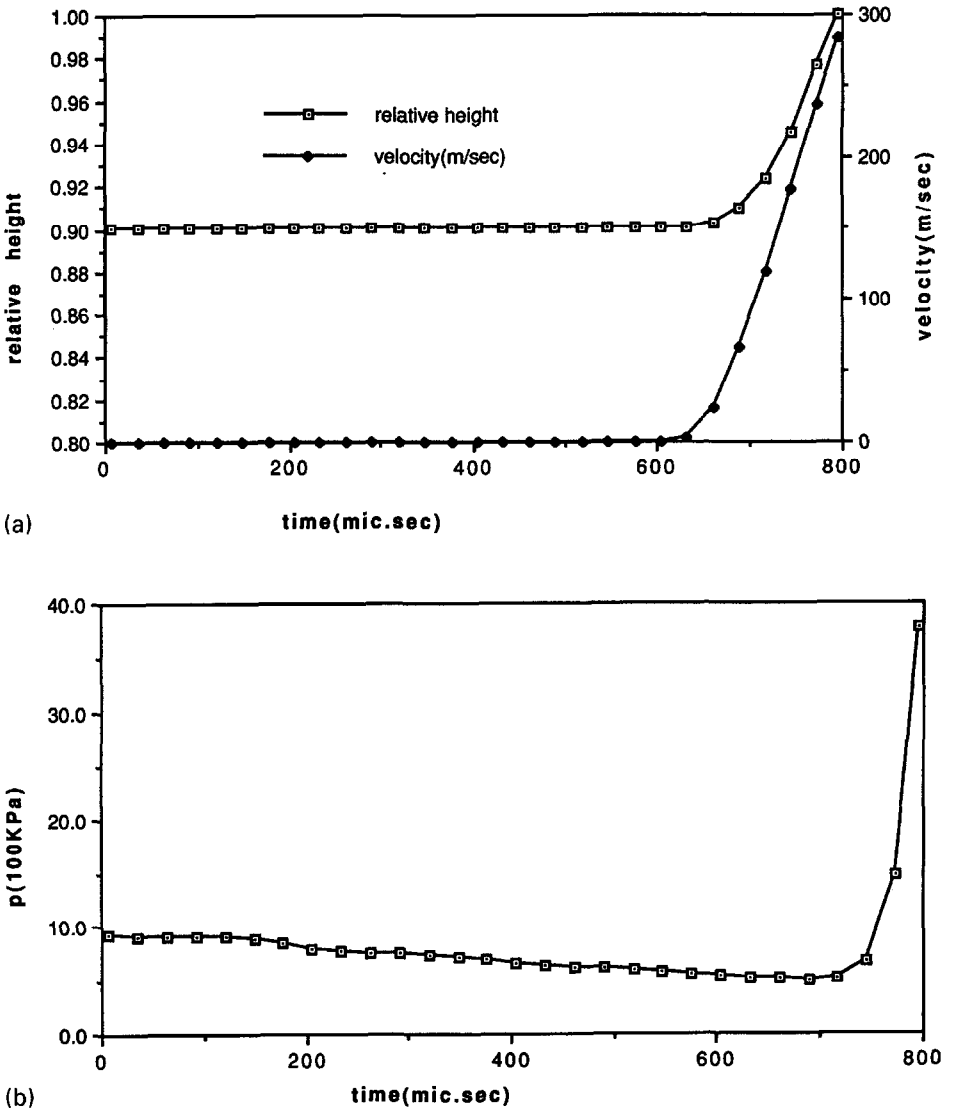

Fig. 9. (a) Variation of interface height and velocity, (b) time variation of pressure at the top of the vessel.

(Fig. 10(b)). These factors are attributable to the fact that the local superheats do not develop to a degree sufficient to initiate the generation of new bubbles.

The distribution of static and dynamic pressures for this event (Fig. 11(a)) and local speed of sound and void fraction (Fig. 11(b)) for this situation further illustrates that the severity of the event depends strongly on initial bubble population and size in addition to local superheat conditions. The void developed (Fig. 11(b)) appears

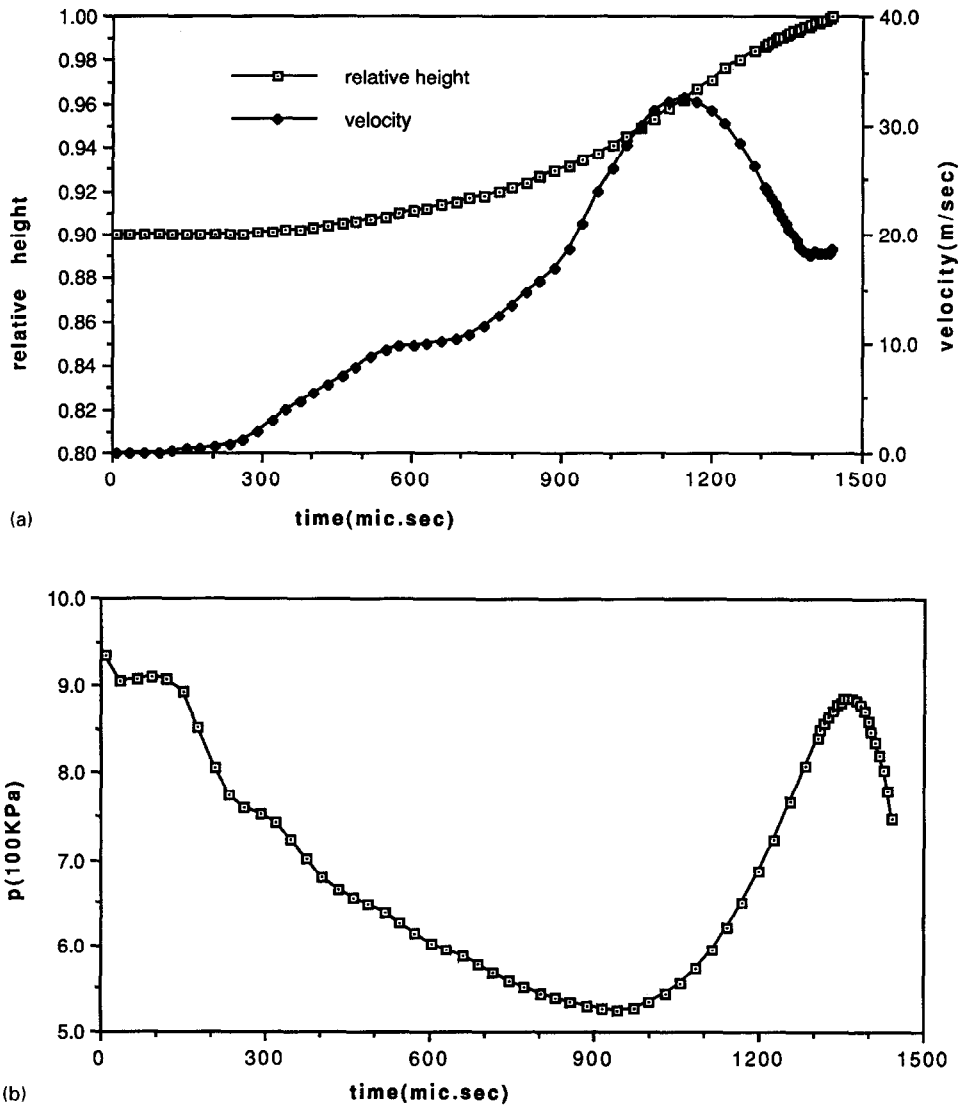

Fig. 10. (a) Variation of interface height and velocity, (b) time variation of pressure at the top of the vessel.

concentrated at the interface ($\alpha \sim 0.3$) and consequently the choke velocity at the crack is low resulting in the possibility of a large dynamic pressure. A BLCBE could be expected from this set of conditions [6].

This point is further clarified by the results shown in Figs. 12 and 13 for an original bubble population ($N_b = 0.5 \times 10^7$ bubbles/cm^3) greater than the previous two cases. Dynamic pressure potential from bubble collapse is significant at the top of the vessel.

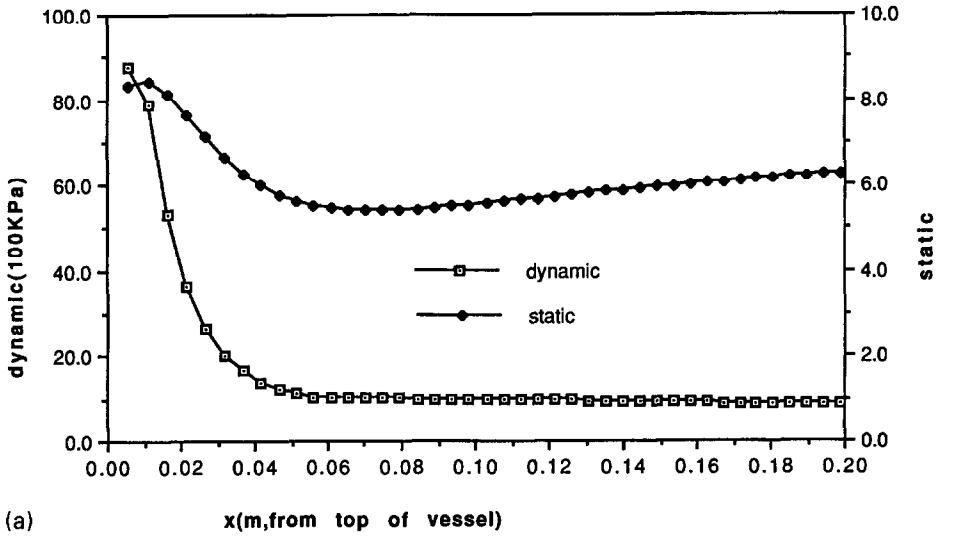

(a)

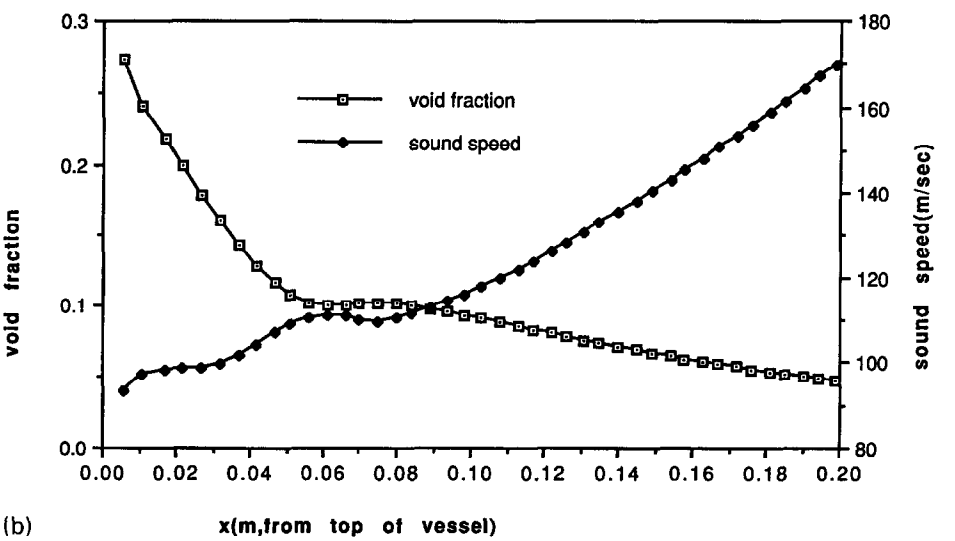

(b)

Fig. 11. (a) Distribution of static and dynamic pressure in the two-phase fluid for a BLCBE, (b) distribution of sound speed and void fraction in the two-phase fluid for a BLCBE.

In this situation swell height develops similar to that shown in Fig. 10(a) although interface velocity peaks earlier to a lower and more constant value (~20 m/s).

Topmost vessel pressure (Fig. 12(b)) and dynamic pressure (Fig. 13(a)) are significantly reduced over those for the previous case (Figs. 10 and 11). The maximum void development in the vessel (Fig. 13(b)) is now concentrated below the interface resulting in a greater crack choke velocity and much lower severity of constraint. A long duration two-phase vent could therefore be anticipated for this event [6].

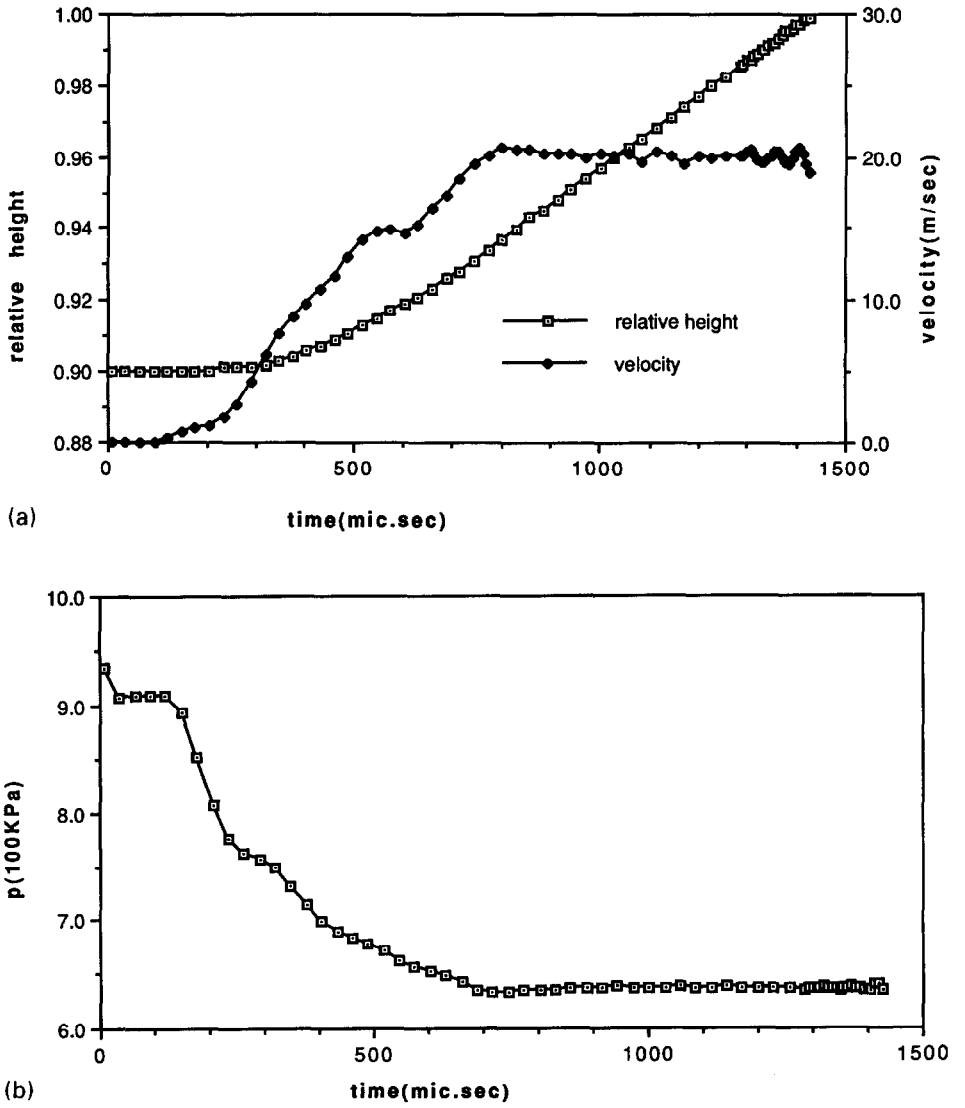

Fig. 12. (a) Variation of interface height and velocity, (b) time variation of pressure at the top of the vessel.

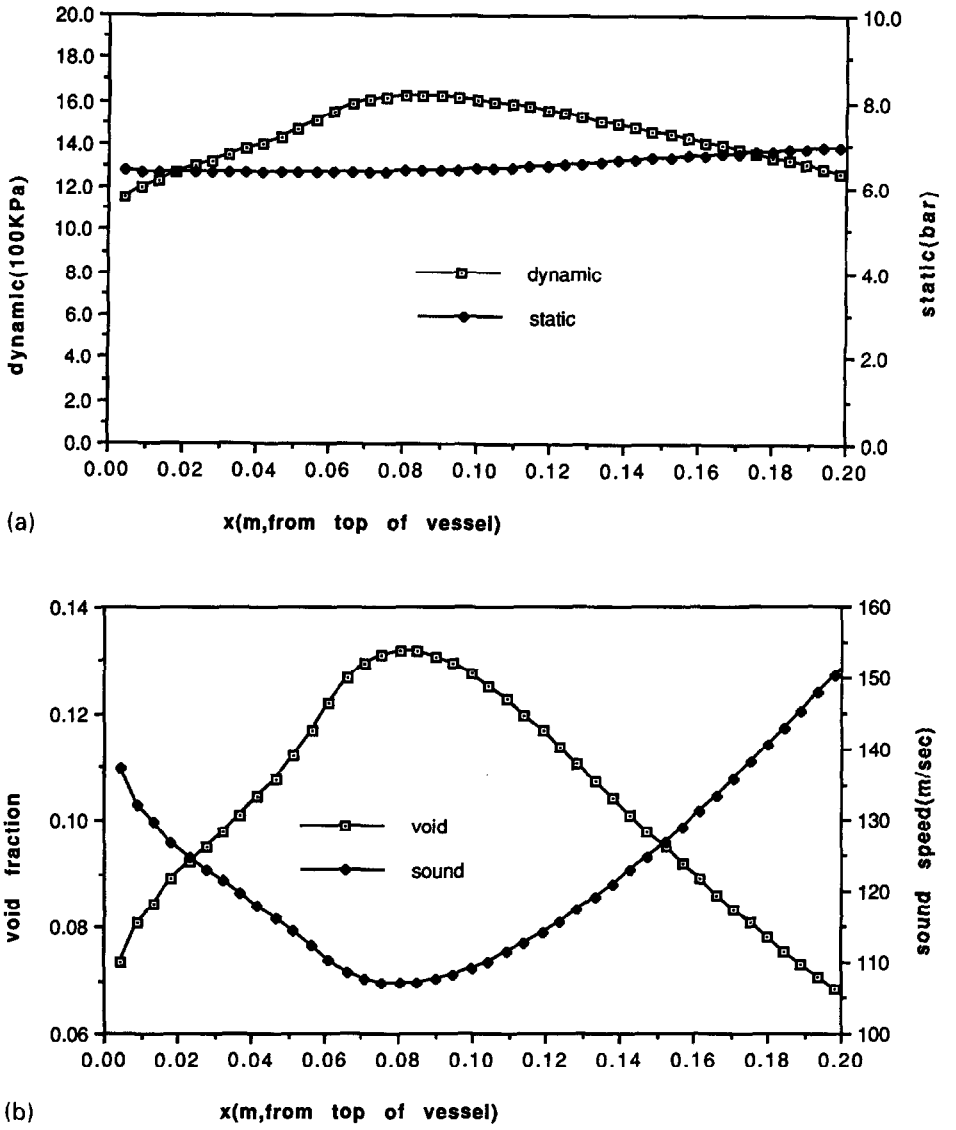

Fig. 13. (a) Distribution of static and dynamic pressures in the two-phase fluid at the vent, (b) distribution of sound speed and void fraction in the two-phase fluid at the vent.

4. Conclusion

1. A preliminary mathematical and physical model along with its associated computer code has been developed and used to predict the types of behaviour for a LOC under several specified conditions. The code may be helpful to recognize,

explain and predict the various types of events possible during accidental LOC of PLG vessels.

2. The model is extremely sensitive to the initial conditions of the liquid lading and in particular the number of bubbles and their position in the liquid. These play a very complex and interactive role in the development of events.

Acknowledgements

Support for this work was provided by the Natural Sciences Engineering Research Council of Canada.

References

[1] N.U. Aydemir, V.K. Magapu, A.C.M. Sousa and J.E.S. Venart, J. Hazard. Mater., 20 (1988) 239.
[2] C.M. Yu and J.E.S. Venart, in: R.W. Lewis, J.H. Chin and G.M. Housey (Eds.), Numerical Methods in Thermal Problems, Vol. II, Part 2, Pinetree Press, Swanse, 1991, pp. 1196–1213.
[3] C.M. Yu and J.E.S. Venart, in: Bu-Xuan Wang (Ed.), Transport Phenomena Science and Technology, High Education Press, 1992, pp. 1028–1034.
[4] J.E.S. Venart, G.Rutledge, K. Sumathipala and K. Sollows, Process Safety Prog., 12(2) (April 1993) 67.
[5] R.C. Reid, Rapid Phase Transitions from Liquid to Vapour, Vol. 12, Advances in Chemical Engineering, Academic Press, 1983, pp. 112–203.
[6] J.E.S. Venart, K.F. Sollows, K. Sumathipala, G.A. Rutledge and X. Jian, Boiling Liquid Compressed Bubble Explosions: Experiments/Models, FED-Vol. 165, Gas–Liquid Flows, ASME, New York, 1993, pp. 55–60.
[7] F.R. Young, Cavitation, McGraw-Hill, London, 1989.
[8] S.V. Stralen and R. Cole, Boiling Phenomena, Vol. 1, Hemisphere, Washington, 1979.